Proc. Schl. Eng. Tokai Univ., Ser. E
40 (2015) 63-70

# Four-Wheel Drive and Independent Steering for Small Electric Vehicles: Active Stability Control during High–Speed Cornering

By

Muhammad Izhar ISHAK[*1], Hirohiko OGINO[*2] and Yoshio YAMAMOTO[*3]

(Received on Mar. 30, 2015 and accepted on Jul. 30, 2015)

**Abstract**

Since car manufacturers pursue in the development of environmental-friendly vehicle, the demand for extensive research on stability, controllability, and reliability of electric vehicles (EVs) increases. Electric-powered and by-wire control technology allow manufacturers to build independent four-wheel steering of an all-wheel drive in-wheel EV. In past research, we investigated the advantages of a four-wheel drive and independent steering system (4WDIS) of an in-wheel small EV in comparison with a two-wheel steering (2WS) vehicle. During low-speed cornering, a 4WDIS in-wheel small EV is capable of cornering with a short radius and has a higher response to driver's steering with the assistance of passive-control rear-wheel steering. This paper describes an active stability control of a 4WDIS in-wheel small EV during high-speed cornering using a numerical simulation. In the simulation, a 4WDIS in-wheel small EV is designed with a nonlinear model. Therefore, a feedback control cannot be implemented directly because the yaw rotational speed couples with the velocity as expressed in the dynamic equation of motion. Hence, we propose controlling the input of a state observer with a controlled linear model enabling the output to be fed forward to the vehicle. A Linear Quadratic Regulator is used to establish an optimal control for the linear model. Based on the result, a slight deviation is observed between the output of the state observer and vehicle model when using the feed-forward control method. As a solution, these output error between both models is calculated and multiplied by a high gain, then fed back into the linear model before the control input is fed forward to the vehicle. Finally, we compare the feed-forward control system with the feedback control system of the vehicle. The results show that our vehicle's active stability control is able to achieve a steady-state cornering at high-speed.

.

***Keywords:*** Four–wheel drive, Independent–steering system, In-wheel small EV, State observer, Linear quadratic regulator

## 1. Introduction

In recent years, electric vehicles (EVs) have renewed the common interest of consumers and manufacturers as they are seen to bring solutions to the environmental concerns over petroleum-based transportation and the issue of fossil fuel depletion around the world. Small EVs for transportation are especially useful in urban areas where spaces are limited. The driving mechanisms of an EV can be divided into two types. The most basic type is the central motor system, where a conventional combustion engine is replaced with an electric motor. The other type is the in-wheel motor system, where a driving motor is located near the hub of each wheel. We believe that the in-wheel motor system has tremendous potential in the future of EVs for its compactness and high energy efficiency[1-4]. In past research, results show that the in-wheel motor system offers more freedom of movement for each wheel and can be governed separately by control systems such as the anti-lock brake system (ABS) and the traction control system (TCS)[5].

As the automotive industry progresses in electric-based transportation, demand increases for better stability, controllability, and reliability of EVs. Some of the mechanical parts of a conventional vehicle will be converted into electric modules that only require signal cables. By combining electric-powered and by-wire control technology, an extensive amount of mechanical parts can be eliminated, enabling then a freedom of layouts and driving potentials. For this reason, an independent four-wheel steering system for EVs becomes much easier to be implemented compared with conventional

*1 Graduate Student, Course of Science and Technology
*2 Professor, Department of Prime Mover Engineering
*3 Professor, Department of Precision Engineering

vehicles.

Vehicles are inherently nonlinear systems and they tend to under-steer at low-speed and over-steer (OS) at high-speed. In the past, we investigated the steering performance of a 4WDIS in-wheel small EV (Toyota COMS as model) under low-speed driving using numerical simulations [6]. The vehicle model produced an OS gradient, which was found to depend on tire-cornering stiffness and length to the center of gravity of the vehicle. With a vehicle in OS, the circular turning radius for a given steering angle vanishes and the yaw angular velocity and the side-slip angle rapidly increases. The purpose of the study was to increase the mobility of a small EV. A passive control system governs the rear steering. At a low speed, the vehicle has a high traction with the road surface and maintains stability, and hence a passive control is considered adequate. As a result, a 4WDIS in-wheel EV is capable of cornering with a shorter cornering radius and has a higher response to the driver's steering.

In this paper, we investigate the active stability control of a 4WDIS in-wheel small EV under high-speed cornering by using numerical simulations. In the simulation, a nonlinear model is employed for the EV. As yaw rotational speed and velocity are coupled, any feedback control (FBC) is incompatible with the nonlinear model. First, it is examined whether the control input of a state observer with a controlled linear model can be fed forward to the non-linear vehicle model. Cornering power for the linear model is achieved by linearizing the side-slip angle verses cornering force for the nonlinear model. A linear quadratic regulator is used to establish an optimal control in the linear model. The output error between the state observer and the vehicle model is calculated and multiplied with a high gain, which is then fed back into the linear model before the control input is fed forward to the vehicle model. The feed-forward control (FFC) system is then compared with the FBC system for the 4WDIS in-wheel small EV. A 4WDIS in-wheel small EV with an active stability can achieve a steady-state cornering at high speed.

## 2. Nomenclature

$b$: width of tire-interaction surface = 0.1 m , $d_F$: front tread = 0.84 m , $d_R$: rear tread = 0.815 m , $I$: yaw inertia moment at the center of gravity of the vehicle = 1470 kgm$^2$ , $K_x$, $K_y$ : tire stiffness = 3.33x10$^6$ N/m$^3$ , $K_F$, $K_R$ : front and rear tire cornering power, $l$: length of tire interaction surface = 0.15 m , $l_F$: length from front axle to the center of gravity of the vehicle = 0.64 m , $l_R$: length from rear axle to the center of gravity of vehicle = 0.64 m , $m$: mass of the vehicle = 421.61 kg , $u$: longitude velocity, $v$: lateral velocity, $X_{FR}$,$X_{FL}$,$X_{RR}$,$X_{RL}$,: friction force for each tire, $Y_{FR}$,$Y_{FL}$,$Y_{RR}$,$Y_{RL}$,: lateral force for each tire, $W_z$: wheels load subject to load transfer, $\beta$, $\beta$*: side-slip angle of vehicle and state observer, $\beta_{FR}$, $\beta_{FL}$, $\beta_{RR}$, $\beta_{RL}$: tire side-slip angle, $\mu$: friction coefficient, $\theta_F$, $\theta_R$ :front and rear tire steer angle, $\gamma$, $\gamma$*: yaw rotational speed of vehicle and state observer, $\rho$: slip ratio, $\omega$ : tire rotational speed.

## 3. Vehicle Dynamics

### 3.1 *Nonlinear model*

A Toyota COMS EV (Fig. 1) is used as a test model in the simulation. Although the vehicle is a 2WD in-wheel EV and has only front-wheel steering, it is configured in simulations with a four-wheel drive and independent steering system.

A general vehicle model has six degrees of freedom: three translational along the $x$, $y$, and $z$-axes, and three rotational about the $x$, $y$ and $z$-axes. In this study, however, a planar motion is assumed so that a translation along the z-axis and rotations about the x and y-axes are disregarded. Fig. 2 depicts the force vector used to construct the dynamic equations of motion for the vehicle and for the yaw rotational speed [7].

The assumption made necessitates us to calculate the dynamic equations for longitude and latitude velocities, including the coupling of the yaw rotation speed with the velocities.

Fig. 1 Toyota COMS EV as a vehicle model

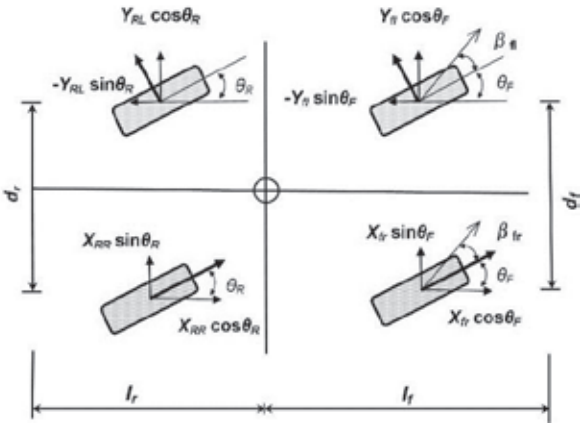


Fig. 2 Vehicle force vectors in four-wheel steering

$$\mathrm{m}\left(\frac{du}{dt}-v\gamma\right)=(X_{FR}+X_{FL})\cos\theta_F+(X_{RR}+X_{RL})\cos\theta_R-(Y_{FR}+Y_{FL})\sin\theta_F-(Y_{RR}+Y_{RL})\sin\theta_R \quad (1)$$

$$\mathrm{m}\left(\frac{dv}{dt}+u\gamma\right)=(X_{FR}+X_{FL})\sin\theta_F+(X_{RR}+X_{RL})\sin\theta_R+(Y_{FR}+Y_{FL})\cos\theta_F+(Y_{RR}+Y_{RL})\cos\theta_R \quad (2)$$

$$\mathrm{I}\frac{d\gamma}{dt}=l_F[(X_{FR}+X_{FL})\sin\theta_F+(Y_{FR}+Y_{FL})\cos\theta_F]+l_R[(X_{RR}+X_{RL})\sin\theta_R+(Y_{RR}+Y_{RL})\cos\theta_R]+\frac{d_F}{2}[(X_{FR}+X_{FL})\cos\theta_F+(Y_{FR}+Y_{FL})\sin\theta_F]+\frac{d_R}{2}[(X_{RR}+X_{RL})\cos\theta_R+(Y_{RR}+Y_{RL})\sin\theta_R] \quad (3)$$

### 3.2 *Nonlinear tire characteristics*

In the simulation, we model the wheels using a brush tire model. Thus, the equations for friction and lateral forces depend on the slip ratio, tire side-slip angle, and weight distribution. The model's deformation of the tire tread rubber is also used to derive the following equations [8],

$$\xi_p=1-\frac{K_\rho\lambda}{3\mu W_z(1-\rho)}\quad,\quad \lambda=\sqrt{\rho^2+\left(\frac{K_\beta}{K_\rho}\right)^2\tan^2\beta}$$

$$K_\rho=\frac{bl_T{}^2}{2}K_x\quad,\quad K_\beta=\frac{bl_T{}^2}{2}K_y$$

If $\xi_\rho \geq 0$,

$$\left.\begin{aligned}X&=-K_\rho\rho\xi_p{}^2-6\mu W_z\frac{\rho}{\lambda}\left(\frac{1}{6}-\frac{1}{2}\xi_p{}^2+\frac{1}{3}\xi_p{}^3\right)\\ Y&=-K_\beta(1+\rho)\tan\beta\,\xi_p{}^2-6\mu W_z\left(\frac{K_\beta\tan\beta(1+\rho)}{K_\rho\lambda}\right)\times\left(\frac{1}{6}-\frac{1}{2}\xi_p{}^2+\frac{1}{3}\xi_p{}^3\right)\end{aligned}\right\} \quad (4)$$

else,

$$\left.\begin{aligned}X&=-\mu W_z\frac{\rho}{\lambda}\\ Y&=-\mu W_z\left(\frac{K_\beta\tan\beta(1+\rho)}{K_\rho\lambda}\right)\end{aligned}\right\} \quad (5)$$

The equation for side-slip angle for each tire is given as follows [9].

$$\left.\begin{aligned}\beta_{FR}&=\tan^{-1}\left(\frac{v+l_F\gamma}{u+d_F\gamma/2}\right)-\theta_F\\ \beta_{FL}&=\tan^{-1}\left(\frac{v+l_F\gamma}{u-d_F\gamma/2}\right)-\theta_F\\ \beta_{RR}&=\tan^{-1}\left(\frac{v-l_R\gamma}{u+d_R\gamma/2}\right)-\theta_R\\ \beta_{RL}&=\tan^{-1}\left(\frac{v-l_R\gamma}{u-d_R\gamma/2}\right)-\theta_R\end{aligned}\right\} \quad (6)$$

The slip ratio $\rho$ can be represented in terms of the traction between the road and the tire surface, which is defined as

$$\rho=\frac{r\omega-u}{r\omega} \quad (7)$$

Then the coefficient of friction $\mu$ can be approximated by the following equation [10].

$$\mu=-1.10\mathrm{k}\times(e^{35\rho}-e^{0.35\rho}) \quad (8)$$

where

$$\begin{cases}k=1.0\ \ (dry\ asphalt)\\ k=0.2\ \ (icy\ road)\end{cases}$$

## 4. State Observer Unit

### 4.1 *Linear model*

The state observer unit uses linear model dynamic equations of the translational motion and yaw rotational motion such as,

$$\mathrm{m}v\left(\frac{d\beta}{dt}+\gamma\right)=2Y_f+2Y_r+G \quad (9)$$

$$\mathrm{I}\frac{d\gamma}{dt}=(2l_fY_f-2l_rY_r-l_GG)\cos\beta \quad (10)$$

It is to be noted that there is no difference in the characteristics of the left and right tires due to linearity, hence, a 2-wheel model is derived from the equations. If the side-slip angle is small, it is assumed that the direction perpendicular to the traveling direction of the vehicle almost coincides with the lateral direction *y*. Therefore, no coupling exists between the yaw rotational speed and the vehicle's translational velocity.

### 4.2 *Linear tire characteristics*

The linear lateral force is defined by

$$Y_f=-K_f\beta_f=-K_f\left(\beta+\frac{l_f}{v}\gamma-\theta_f\right) \quad (11)$$

$$Y_r=-K_r\beta_r=-K_r\left(\beta-\frac{l_r}{v}\gamma-\theta_r\right) \quad (12)$$

Here, the cornering power of the front and rear wheels, $K_F$ and $K_R$, are obtained from the tangent at the origin for the plot of side-slip angle verses cornering force in the nonlinear vehicle

model. In contrast, with the tire characteristics of the nonlinear model, the actual vehicle motion determines the linear model lateral forces, which are related to the side-slip angle, yaw rotational speed, and front and rear steering angles.

The above equations can be substituted into the linear dynamic equations of motion eq. (9) and the yaw rotational speed eq. (10).

### 4.3 *Linearized differential equation*

The linearized differential equation represents the linear vehicle dynamic equation of motion for the state observer. It is arranged as a set of first-order ordinary differential equations in the vector state form:

$$\left.\begin{aligned} \dot{\mathrm{x}} &= \mathrm{Ax} + \mathrm{BU}_r + \mathrm{CU}_f \\ y_\beta &= \beta^* = {\mathbb{C}_1}^T \mathrm{x} \\ y_\gamma &= \gamma^* = {\mathbb{C}_2}^T \mathrm{x} \end{aligned}\right\} \quad (13)$$

$$\mathrm{x} = [\beta^* \quad \gamma^*]^T,$$
$${\mathbb{C}_1}^T = [1 \quad 0]^T, \qquad \mathrm{U}_f = \theta_F,$$
$${\mathbb{C}_2}^T = [0 \quad 1]^T, \qquad \mathrm{U}_r = \theta_R,$$

$$\mathrm{A} = \begin{bmatrix} a & b \\ c & d \end{bmatrix} = \begin{bmatrix} -\dfrac{2(K_f + K_r)}{mv} & -1 - \dfrac{2(K_f l_f - K_r l_r)}{mv^2} \\ -\dfrac{2(l_f K_f - l_r K_r)}{I} & \dfrac{2({l_f}^2 K_f + {l_r}^2 K_r)}{Iv} \end{bmatrix},$$

$$\mathrm{B} = \begin{bmatrix} e \\ f \end{bmatrix} = \begin{bmatrix} \dfrac{2K_r}{mv} \\ -\dfrac{2l_r K_r}{I} \end{bmatrix}, \qquad \mathrm{C} = \begin{bmatrix} k \\ l \end{bmatrix} = \begin{bmatrix} \dfrac{2K_f}{mv} \\ \dfrac{2l_f K_f}{I} \end{bmatrix},$$

The state vector x represents the side-slip angle and yaw rotational speed of the vehicle. The steering angles of the front and rear wheels are the inputs of this system. The value for the front-wheel angle $\theta_F$ is a driver-selected input whereas the rear-wheel angle $\theta_R$ is initially 0 degrees. During high-speed cornering, the rear-wheel steering is used as the control input by introducing a feedback gain $-g^T$.

$$\mathrm{U}_r = -g^T \mathrm{x} + \theta_R \quad (14)$$

### 4.4 O*ptimal control*

To find the optimal control for the linearized differential equation, the following evaluation function $J$ is employed.

$$\begin{aligned} J &= \int_0^\infty (q_{11}\beta^{*2} + q_{22}\gamma^{*2} + w\theta_r^2)dt \\ &= \int_0^\infty (\mathrm{x}^T Q \mathrm{x} + w\theta_r^2)dt \end{aligned} \quad (15)$$

where

$$\mathrm{Q} = \begin{bmatrix} q_{11} & 0 \\ 0 & q_{22} \end{bmatrix}$$

in which $q_{11}$, $q_{22}$, and $w$ are appropriately chosen constant weighting matrices for the side-slip angle, yaw rotational speed, and rear-wheel steering angle, respectively. The optimal solution for $J$ can be designed if Q is a positive definite matrix and the state observer control input $\mathrm{U_r}$ is given by

$$\mathrm{U}_r = -\frac{1}{r} B^T P \mathrm{x} + \theta_R \quad (16)$$

where

$$-\mathrm{g}^T = -\frac{1}{r} B^T P$$

With $\mathrm{P} = \mathrm{P}^T \geq 0$ being the unique positive-semidefinite solution of the algebraic Riccati equation,

$$A^T \mathrm{P} + \mathrm{PA} - w^{-1} PBB^T P = -Q$$

or

$$\begin{bmatrix} a & b \\ c & d \end{bmatrix}^T \mathrm{P} + \mathrm{P} \begin{bmatrix} a & b \\ c & d \end{bmatrix} - w^{-1} \mathrm{p} \begin{bmatrix} e \\ f \end{bmatrix} [e \quad f]^T \mathrm{P} = -\begin{bmatrix} q_{11} & 0 \\ 0 & q_{22} \end{bmatrix} \quad (17)$$

where P is given as,

$$\mathrm{P} = \begin{bmatrix} \varepsilon & \phi \\ \psi & \epsilon \end{bmatrix}$$

## 5. 4WDIS Stability Control System

### 5.1 *Feed-forward control system*

Figure 3 shows the diagram of the FFC for a 4WDIS in-wheel small EV. In this system, the angle of the front wheel $\theta_F$ is relayed to the state observer unit from the driver. The state observer unit estimates the yaw rotational speed and side-slip angle output, evaluating them via the aforementioned optimal control method, to produce the control input $U_r$. The control input is then fed forward to the nonlinear vehicle model.

### 5.2 *Feedback control system*

The FFC system for the 4WDIS in-wheel small EV can be considered to have low precision. Some error in the output results between the vehicle's nonlinear model and the state observer's linear model is expected. Fig. 4 shows the FBC system for a 4WDIS in-wheel small EV using error elimination. To minimize the error oscillation, the estimated yaw rotational speed output of state observer unit and the measured yaw rotational speed output of the vehicle model are compared then multiplied by high gain $H$. Then, this gain is fed back into the linear model. The linearized differential equation of eq. (13) becomes

$$\left.\begin{aligned} \dot{\hat{\mathrm{x}}} &= \mathrm{Ax} + \mathrm{BU}_r + \mathrm{CU}_f + H\tilde{r} \\ \tilde{r} &= \gamma - \gamma^* = {\mathbb{C}_2}^T \hat{\mathrm{x}} - {\mathbb{C}_2}^T \mathrm{x} \\ &= {\mathbb{C}_2}^T (\hat{\mathrm{x}} - \mathrm{x}) \end{aligned}\right\} \quad (18)$$

The renewed state observer control input can also be redefined,

$$U_r = -\frac{1}{r}B^T P(\hat{x} - x) + \theta_R \qquad (19)$$

With this equation, the FFC for the 4WDIS in-wheel small EV can be changed to a FBC that gives greater precision.

## 6. Simulation Procedure

To determine the cornering power needed to design the state observer, the first procedure of the simulation is to simulate a cornering condition for the nonlinear 4WDIS in-wheel EV at a constant speed (u = 15 km/h) and constant front and rear steering angles of 10 degrees.

After obtaining the cornering power, a state observer unit with the optimal control is determined. The control input from the state observer is fed forward to the nonlinear vehicle model (Fig. 3). Then, a high-speed cornering condition is simulated. In this cornering condition, the vehicle constant velocity is set to 50 km/h and the front-wheel steering angle is set to 10 degrees, which is initiated at t = 10 s (at a constant velocity). The maximum time duration of the simulation is 40 s. A 2WS

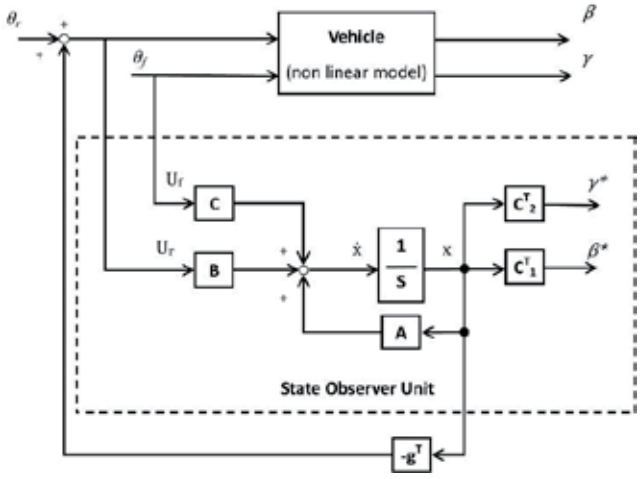


Fig. 3 Feedforward control system for 4WDIS in-wheel small EV

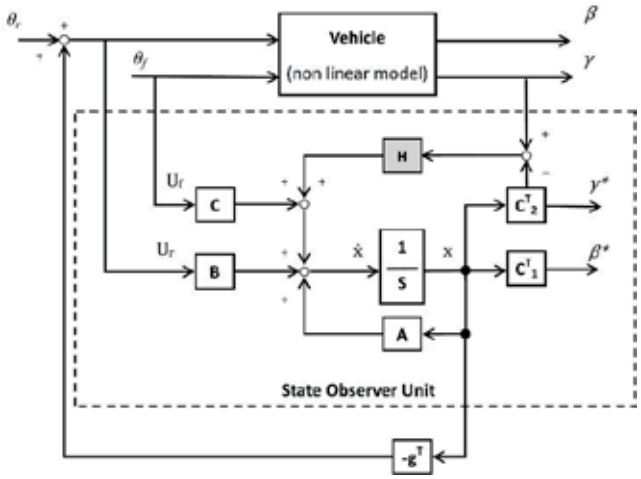


Fig. 4 Feedback control system for 4WDIS in-wheel small EV

in-wheel small EV without the stability control is also simulated under the same condition.

In the next simulation, the FFC system is developed to improve the results. The yaw rotational speed output between the vehicle and the state observer unit are compared and calculated as output error. Then, this error is multiplied by the high gain. This result is then relayed back to the state observer unit. The rectified control input is fed into the nonlinear vehicle model (Fig. 4). The previous simulation subject to the high-speed cornering condition is repeated again.

## 7. Results and Discussions

### 7.1 *Identification of cornering power*

Figure 5 shows the relationship between the side-slip angle and the cornering force of each tire for the nonlinear model of the 4WDIS vehicle that is produced from the first simulation of cornering at a low-speed and constant front and rear steering angles. The cornering power is determined from the tangent of the plot at the origin. We find the cornering power for the front and rear wheels $K_F$ and $K_R$ to be 1200 N/rad, which is then used to construct the linear model for the state observer unit.

### 7.2 *High-speed cornering of 4WDIS EV with feed-forward control in comparison with 2WS*

Figure 6 shows the trajectory of the 4WDIS vehicle with FFC, the state observer unit, and the 2WS vehicle with no control during high-speed cornering. The black solid and broken lines represent the 4WDIS vehicle and the state observer unit, respectively, whereas the gray line represents the 2WS vehicle. The trajectory of the state observer unit is estimated based on the output values.

Figure 7 shows the front and rear-wheel steering angles in radians. The black line represents the front steering angle, which is the steering input chosen by the driver, whereas the grey line represents the rear steering angle, which is the control input produced by the state observer unit.

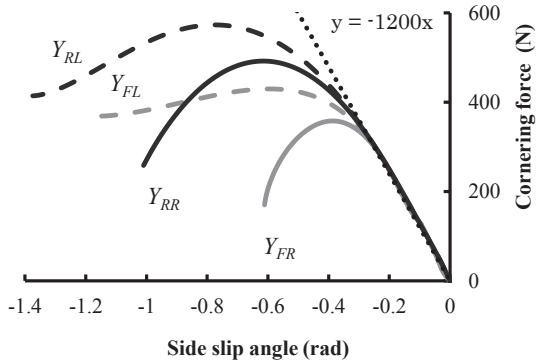


Fig. 5 Relation between the lateral force and the side-slip angle of the 4WDIS vehicle

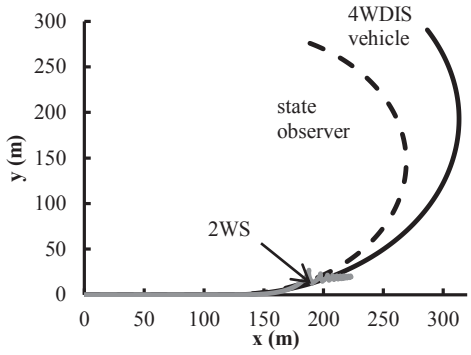


Fig. 6 Trajectory of 4WDIS vehicle, state observer, and 2WS vehicle during high-speed cornering

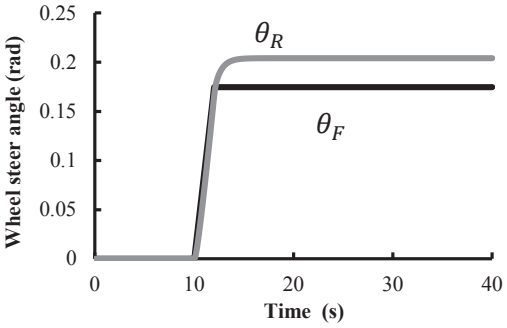


Fig. 7 Front and rear wheel steer angle

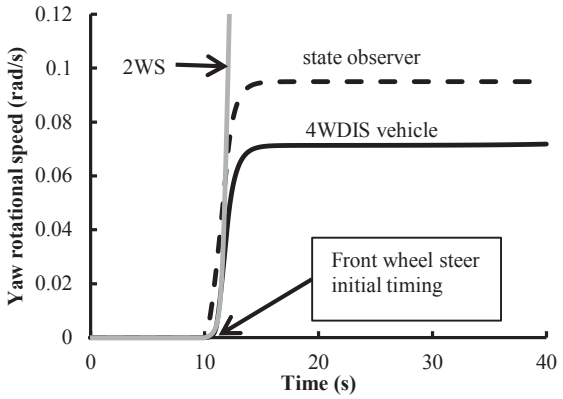


Fig. 8 Comparison of yaw rotational speed

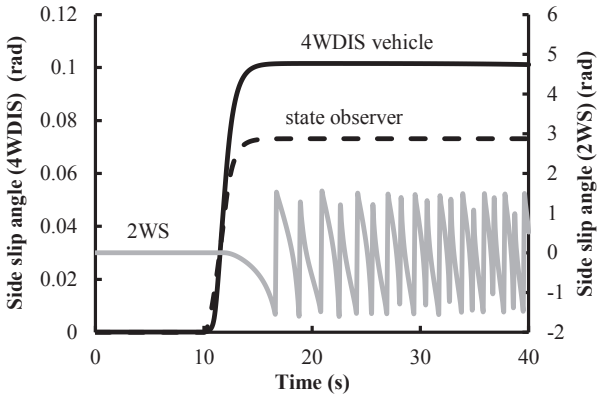


Fig. 9 Comparison of side slip angle at center gravity

The purpose of the simulation for a 2WS vehicle is to demonstrate that without a stability control system, cornering at a high-speed is impossible. For a 2WS vehicle, there is no stability control system applied and only the front wheels produces a steering angle. Based on the plot of the trajectory, the vehicle does not travel far and shows an evidence of over-steer and instability.

However, for the 4WDIS vehicle, the trajectory shows a circular motion, which indicates that the vehicle is able to make a turn with the assistance of FFC from the state observer unit. Nevertheless, dissimilarities are evident in the cornering characteristic between the 4WDIS vehicle and the state observer unit. The 4WDIS vehicle exhibits a larger turning radius compared with the state observer.

These variations in trajectory can be explained from the graphs of the yaw rotational speed (Fig. 8) and side-slip angle (Fig. 9) for the 4WDIS vehicle with FFC, the state observer unit, and the 2WS vehicle with no control. Again, the black solid and broken lines represent results for the 4WDIS vehicle and the state observer unit, respectively, whereas the gray line represents that for the 2WS vehicle. In Fig. 9, the left ordinate gives the scale of the side-slip angle for the 4WDIS vehicle and state observer unit and the right ordinate gives the scale for the 2WS vehicle.

For 2WS, as soon as steering is initiated at t = 10s, the yaw rotational speed accelerates rapidly. The side-slip angle of the 2WS vehicle shows an oscillation between -2.0 and 2.0 rad. We confirm the earlier hypothesis that the 2WS vehicle over-steers during a high speed cornering.

In contrast, if a vehicle has 4WDIS FFC implemented, the yaw rotational speed and side-slip angle maintain constant values. In general, if a front-wheel steering angle is initiated, the vehicle will produce a yaw motion. In our case, the state observer unit evaluates the yaw rotational speed output and produces a rear steering angle as a control input to achieve steady-state cornering even at high-speeds. The rear steering angle $\theta_R$ in Fig. 7 shows a constant angle of 0.2 rad, which is equivalent to 11.5 degrees.

However, in comparison with the output of the state observer unit, the 4WDIS vehicle indicates a lower yaw rotational speed by a margin of –0.024 rad/s and higher side-slip angle by a margin of 0.03 rad. These discrepancies cause the deviation of the measured 4WDIS vehicle and the estimated trajectory of the state observer in Fig. 6.

### 7.3 *Improvement of the active stability control of 4WDIS EV with FBC by error elimination*

In conventional vehicles, there is no other method to measure the value of its side-slip angle. However, yaw rotational speed of a vehicle can be calculated using gyro

sensors. To eliminate the error mentioned above, the estimated output of the state observer unit and the measured output of the nonlinear vehicle model are compared and multiplied by high gain *H*. Then, this gain is fed back to the linear model to produce a rectified control input, which is then transferred to the vehicle.

Figure 10 shows the improvement in yaw rotational speed and Fig. 11 that for the side-slip angle of the 4WDIS vehicle for both the FFC and FBC systems. The gray broken and solid lines represent the state observer and 4WDIS vehicle with a FFC system, whereas the black broken and solid lines represent the state observer and 4WDIS vehicle with FBC system, respectively. The black broken line is not visible because it overlaps with the black solid line.

After applying FBC by error elimination and high gain, the yaw rotational speed of 4WDIS vehicle is now similar to the state observer. The vehicle response to the driver input has also improved. From Fig. 10, an immediate vehicle yaw motion is generated as soon as the front-wheel steering angle is initiated at t = 10 s.

Nevertheless, only the error measurements of yaw rotational speeds are taken into account in the FBC; the side-slip angle of the vehicle is also reduced. Increasing the yaw rotational speed alters the angle of the vehicle's actual traveling direction and the heading direction, thereby reducing the side-slip angle, simultaneously.

Finally, Fig. 12 shows the effect of the output error to the rear-wheel steering angle of the FBC system in comparison with rear-wheel steering angle of the FFC system. For the FFC system, the steering angle of the rear wheel increases depending on the state observer unit control input, which gives a negative output error. However, for the FBC system, the negative output error times the high gain produces a rectified control input. The negative output error delays the input of the steering angle of the rear wheel and enables the 4WDIS vehicle to boost yaw rotational speed via only the front-wheel steering angle until the output error between vehicle and state observer becomes small or approximately zero.

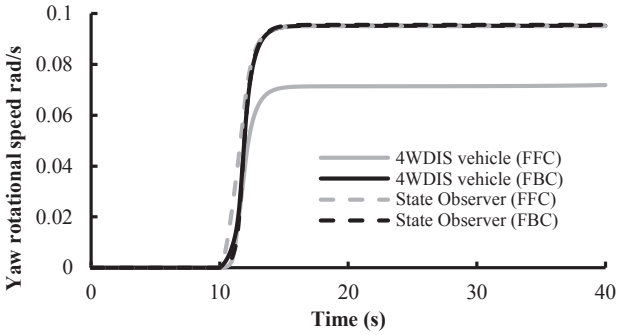


Fig. 10 Comparison of yaw rotational speed for a 4WDIS vehicle and state observer with FFC and FBC systems

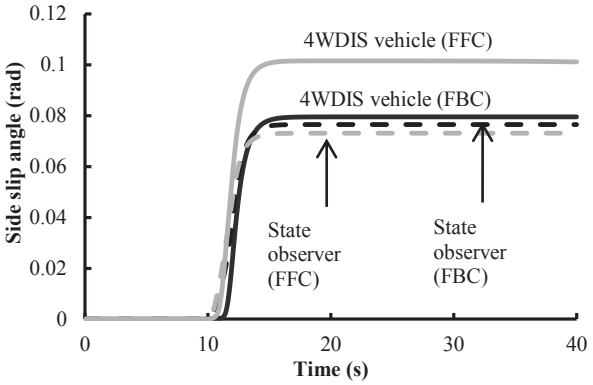


Fig. 11 Comparison of side-slip angle for a 4WDIS vehicle and state observer with FFC and FBC systems

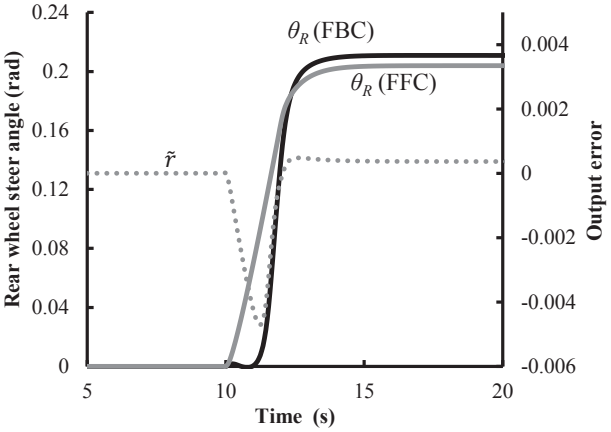


Fig. 12 Effect of the output error on the rear-wheel steering angle and output error of the yaw rotational speed

## 8. Conclusion

An active stability control of a 4WDIS in-wheel small EV was accomplished with FBC using an error elimination system. It is possible that a state observer with a controlled linear model can be fed forward to a vehicle using nonlinear control modeling. However, an actual vehicle is inherently a nonlinear dynamic system, especially during high-speed cornering. Deviations can potentially occur between the outputs of a linear state observer and a nonlinear vehicle model when using the FFC method.

To increase the precision of the active stability system, the output of the actual vehicle and the internal system needs to be unified. When such unification is achieved, a unique control input can be generated to the vehicle to achieve stability.

It is considered that because of high gain, if the nonlinear features inherent in all vehicles can be controlled with this 4WDIS active stability control system, a linear feature can

also be managed during low-speed. Further studies will be needed on whether this 4WDIS control system may have robust characteristics against disturbances.

**Reference**


1) Ssu-Hsin Yu, John J.Moskwa, “A Global Approach to Vehicle Control: Coordination of Four Wheel Steering and Wheel Torques”, Journal of Dynamic Systems, Measurement, and Control (1994), Vol.116, pp.659-667.
2) S. Sano, Y. Furukawa and S. Shiraishi, “Four Wheel Steering System with Rear Wheel Steer Angle Control as a Function of Steering Wheel Angle”, SAE World Congress and Exhibition, Detroit, MI, USA, February 1986, SAE Paper no.860625.
3) Shout, M.A. Jarrah, H. Al-Araji, K.Al-Tell, “A Nonlinear Optimal Four Wheels Steering Controller”, Proceeding of 43rd IEEE Midwest Symposium on Circuits and System, Lancing MI, August 2000, pp.1426-1429.
4) Ministry of Land, Infrastructure and Transport Department of Municipal Affairs and automobile station, "Towards the realization of a new social life through the development and utilization of new (mobility) guidelines for the introduction of ultra-small mobility", http: //www.mlit.go.jp / common / 000212867.pdf, June 24, 2010.
5) Muhammad Izhar Ishak, “Research on Anti-Lock Brake System of A 4WD Small Electric Vehicle with Hydraulic-Mechanical Hybrid Brake System”, International Conference for Young Engineers 2011, Japan.
6) M.Izhar, H.Ogino, Y.Oshinoya, “Inroduction on Dynamic Motion of Opposite and Parallel Steering for electric vehicle”, 2013 IEEE Conference on System, Process & Control (ICSPC), 13-15 Dec 2013, pp. 73-78.
7) Masato Abe, “Automotive Vehicle Dynamics: Theory and Application (vehicle motion for driving and braking)”, Tokyo Denki University Publication (2008), pp.181-182.
8) Masato Abe, “Automotive Vehicle Dynamics: Theory and Application (Tire Dynamics)”, Tokyo Denki University Publication (2008), pp.34-37.
9) Masato Abe, “Automotive Vehicle Dynamics: Theory and Application (Tire Dynamics)”, Tokyo Denki University Publication (2008), pp.54.
10) Yoichi Hori, “Future Vehicle Driven by Electricity and Control (Research on Four Wheel Motored “UOT Electric March II)”, AMC’02 7th International Workshop on Advanced Motion Control, Moribor, Slovenia.